ChemElectroChem

Supporting Information

Electroless Nanoplating of Iridium: Template-Assisted Nanotube Deposition for the Continuous Flow Reduction of 4-Nitrophenol

Martin Christoph Scheuerlein,* Falk Muench, Ulrike Kunz, Tim Hellmann, Jan P. Hofmann, and Wolfgang Ensinger

License: CC BY-NC-ND 4.0 International - Creative Commons, Attribution, NonCommercial, NoDerivs

Supporting Information

Table of contents:

1. Additional UV-Vis spectra of $IrCl_3$ solutions

To better understand the spectral influences of chlorinated Ir complexes and IrO_2 precipitates, UV-Vis reference spectra of 5 mM $IrCl_3$ dissolved in 10 M HCl and 0.1 M NaOH were recorded after heat treatment (**Figure S1**). When 10 M HCl is used as solvent, the formation of chloride-dominated Ir(III) and Ir(IV) complexes is expected.[1] In case of alkaline media, hydrolysis of $IrCl_3$ leads to the precipitation of insoluble IrO_2, resulting in prominent absorption around 570-590 nm.[2,3]

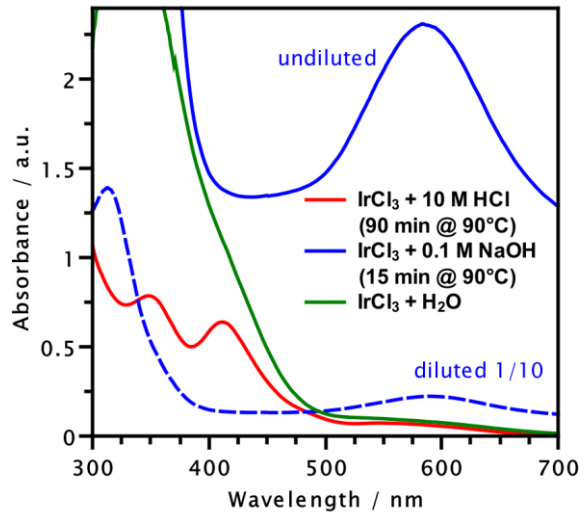

Figure S1: UV-Vis spectra of 5 mM $IrCl_3$ dissolved in 10 M HCl (red line), 0.1 M NaOH (blue lines) and H_2O (green line).

2. Additional XPS detail spectra

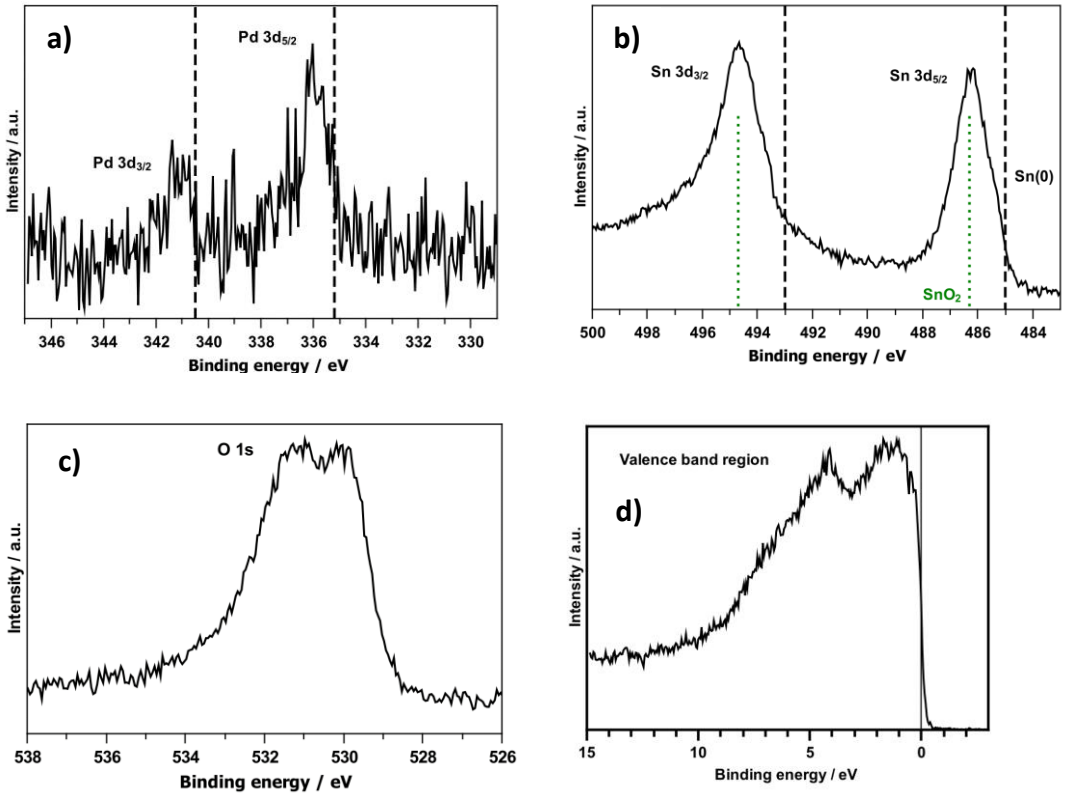

Figure S2: Detailed XPS spectra of the Pd 3d (a), Sn 3d (b), O 1s (c) and valence band (d) regions. Peak positions for Sn(0), SnO_2 and Pd(0) according to [4], [5] and [6], respectively.

Similar to Ir, all other main elements involved in the nanostructure synthesis can be detected in XPS. Interestingly, the intensity of Pd peaks is surprisingly low, considering the abundance of Pd in the EDS spectra (**Figure S2a**), indicating that almost all Pd seeds are covered by an Ir layer, lowering the photoelectron yield. The Sn 3d peaks are shifted to higher binding energies (**Figure S2b**), indicating the formation of oxidized tin species during the synthesis.[4,5] The Pd 3d peaks are difficult to analyze due to their low intensity. However, they also seem slightly shifted to higher binding energies,[6] suggesting that some changes in the chemical environment of the Pd atoms occurs during synthesis. The O 1s peak (**Figure S2c**) is rather wide and probably originates mostly from metal oxides. The electronic structure in the valence band region (**Figure S2d**) corresponds well with a previous report on metallic Ir surfaces.[7] Meaningful contributions from Pd in this range are not expected, due to the overall very low intensity of the Pd photoelectron signal.

Ir film thickness approximation: It is not possible to determine the Ir film thickness using the standard method for XPS, where the attenuation of the substrate signal is assumed to follow a Beer-Lambert law-like relation, since it would require to know the intensity of the Pd 3d emission line without any overcoating as reference value. However, since the intensity of the Pd 3d emission is extremely low (Figure SI2a), it can be assumed that the thickness of the Ir layer is in the range of three times the inelastic mean free path of a Pd 3d photoelectron travelling through the Ir layer. Using the relation of Seah *et al.*,[8] the mean free path of an electron with a kinetic energy of 1150 eV is estimated to be 2.12 nm, which results in a thickness of the Ir film of roughly 6 nm.

3. Catalytic performance in methyl orange degradation

The degradation of methyl orange (MO) was applied as a second model reaction to characterize the catalytic performance of the synthesized catalysts. The course of the reaction can be easily followed using UV-Vis spectrometry, as MO shows a prominent absorbance band centered around 460 nm. For the reaction solution, 5 ml of a 200 µM solution of MO were mixed with an equal amount of freshly prepared 20 mM $NaBH_4$ solution. Catalysis was then performed both in a flow reactor configuration, similar to the experiments with 4-nitrophenol, as well as "statically" with the membrane submerged in a stirred reaction solution. **Figure S3a** shows the UV-Vis spectra of the solution before and after passing the membrane at a flow rate of ~5 ml/min. A conversion of ~93% was observed with both deposits, indicating very high catalytic activity. Similar to the 4-nitrophenol experiments, both deposits show remarkably similar catalytic performance. For that reason, time dependent measurements of MO absorbance were performed only on the citrate-deposit, yielding an apparent rate constant of k_{app} = 0.059 min^{-1} (**Figure S3b**), assuming pseudo-first-order kinetics. Similar to the 4-nitrophenol experiments, the conversion appears to be much slower compared to the flow reactor setup.

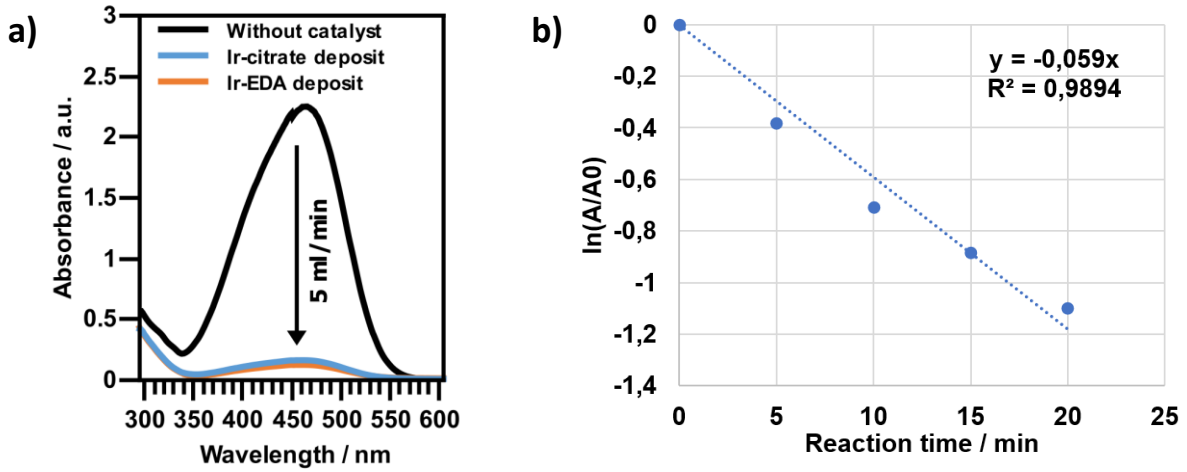

Figure S3: a) UV-Vis spectra of MO/NaBH4 solution before (black line) and after (blue and orange line) passing the Ir catalyst membrane at a flow rate of 5 ml min^{-1}. b) Relative absorbance change over reaction time, yielding an apparent rate constant of 0.059 min^{-1} for the Ir-citrate deposit.

4. Surface area calculations

A simple geometrical model is applied to relate the surface of the cylindrical pore walls to the total surface of the catalyst membrane. The pore diameter *d*, pore density *D* and membrane thickness *t* are taken from the manufacturer specifications (**Equation 1**) and the orientation of the pores is assumed to be perfectly perpendicular with respect to the membrane surface.

$$d_p = 400\ nm; D = 1.5 \cdot 10^8\ cm^{-2}; t = 25\ \mu m \tag{1}$$

Assuming cylindrical pores, the inner surface of one pore can be calculated as follows (**Equation 2**).

$$\pi \cdot d_p \cdot t \approx\ 3.1416 \cdot 10^{-7} cm^2 \tag{2}$$

For a circular membrane with a diameter of $d_{total} = 1.3\ cm$, the total inner surface of all pores A_p can be calculated using **Equation 3**.

$$A_P = \pi^2 \cdot d_p \cdot t \cdot D \cdot \left(\frac{d_{total}}{2}\right)^2 \approx 62.549\ cm^2 \tag{3}$$

The total surface of the membrane A_{total} additionally includes the top and bottom areas of the membrane foil as well as the lateral surface of the circular membrane, minus the areas of the pore openings (**Equation 4**).

$$A_{total} = A_p + 2\pi \left(\frac{d_{total}}{2}\right)^2 + \pi \cdot d_{total} \cdot t - \pi \left(\frac{d_p}{2}\right)^2 \cdot D \approx 64.953\ cm^2 \tag{4}$$

It follows, that the inner pore surfaces make up ~96.3% of the total catalyst membrane surface (**Equation 5**).

$$\frac{A_p}{A_{total}} \cdot 100\% \approx 96.3\% \tag{5}$$

5. References

[1] J. G. H. du Preez, C. Viviers, T. Louw, E. Hosten, H. Jonck, *Solvent Extr. Ion Exch.* **2004**, *22*, 175–188.

[2] Y. Zhao, E. A. Hernandez-Pagan, N. M. Vargas-Barbosa, J. L. Dysart, T. E. Mallouk, *J. Phys. Chem. Lett.* **2011**, *2*, 402–406.

[3] D. Xu, P. Diao, T. Jin, Q. Wu, X. Liu, X. Guo, H. Gong, F. Li, M. Xiang, Y. Ronghai, *ACS Appl. Mater. Interfaces* **2015**, *7*, 16738–16749.

[4] J. F. Moulder, W. F. Stickle, P. E. Sobol, K. D. Bomben, *Handbook of X-Ray Photoelectron Spectroscopy*, Physical Electronics Inc., Eden Prairie, **1995**.

[5] M. A. Stranick, A. Moskwa, *Surf. Sci. Spectra* **1993**, *2*, 50–54.

[6] M. C. Militello, S. J. Simko, *Surf. Sci. Spectra* **1994**, *3*, 387–394.

[7] R. Koetz, H. Neff, S. Stucki, *J. Electrochem. Soc.* **1984**, *131*, 72–77.

[8] M. P. Seah, W. A. Dench, *Surf. Interface Anal.* **1979**, *1*, 2-11.